Widely Tunable Femtosecond Soliton Pulse Generation by Using Soliton-Frequency Shift in a Photonic Crystal Fibre *

CHENG Chun-Fu(成纯富)**, WANG Xiao-Fang(王晓方), SHEN Bai-Fei(沈百飞)

Laboratory for High Intensity Optics, Shanghai Institute of Optics and Fine Mechanics, Chinese Academy of Sciences, Shanghai 201800

(Received 10 May 2004)

Femtosecond Raman soliton generation, tunable from 800 to 1044 nm, has been theoretically investigated for a photonic crystal fibre pumped by a 200-fs pulse. A highly nonlinear photonic crystal fibre with a length of only 57.7 cm and a nonlinear coefficient of 0.075 $(Wm)^{-1}$ is used to achieved such a broadband. It is found that the spectral bandwidth increases with the input peak power. In particular, it is also found that the output wavelengths of the resulting sub-40 fs Raman solitons can also be tuned effectively by varying the initial pulse chirp. There exists an optimal positive chirp which maximizes the bandwidth, corresponding to the formation of only one long-wavelength Raman soliton.

PACS: 42. 65. Re, 42. 81. Dp, 42. 72. Ai

Photonic crystal fibres (PCFs) have attracted significant attention because of their unusual optical properties and their large potential for important applications. A PCF consists of a fused silica core surrounded by an ordered array of microscopic air holes running along its length. The air holes form a low-index cladding around the solid-silica core; therefore the light is guided by total internal reflection as in standard step-index fibres. The large difference of refractive-index between the 1–3 μm diameter core and the holey cladding provides a very strong specifically controlled waveguide contribution to dispersion. Therefore the optical properties of a PCF differ remarkably from those of standard fibres. In particular, the zero-dispersion wavelength can be shifted into the visible region.[1] A PCF can show single-mode operation over almost the complete transmission range.[2] Due to their novel guidance properties and enhanced nonlinearity, PCFs have already been widely exploited in applications such as dispersion compensation,[3] optical frequency metrology,[4] and optical coherence tomography.[5] An important recent advance is the development of tapered PCFs in which the soliton self-frequency shift (SSFS) caused the generation of tunable Raman solitons at telecommunication wavelengths around 1300–1600 nm.[6] These solitons would be suitable for many applications in telecommunications, such as multiterabits/s optical time-domain multiplexing and wavelength division multiplexing transmission, and so on.

With SSFS, wavelength shifting from 1.56 to 1.78 μm was demonstrated for 180-fs, 48-Mhz pulses in a 75-m-long normal fibre.[7] Furthermore, shifting of the wavelength from 1.56 to 2.13 μm has been achieved for 350-fs pulses in a 70-m-long fibre.[8] As can be seen, the use of conventional fibres to generate frequency-shifting solitons is limited by the zero dispersion wavelength and the usually large effect of cubic dispersion.[7–9] However, the required fibre length can be reduced significantly by the use of the PCF with high nonlinearity. In this Letter, a theoretical investigation on the nonlinear pulse propagation and tunable femtosecond Raman soliton generation in the anomalous dispersion region of a PCF with a core diameter of 2 μm pumped by a 200-fs pulse is presented. It is found the output wavelength can be widely tuned by varying the input peak power or the initial pulse chirp and we obtained solitons with a sub-40-fs width, tunable from 800 to 1044 nm within an only 57.5 cm long but highly nonlinear PCF. It is also found that positive chirps enhance the spectral bandwidth while negative chirps suppress the spectral bandwidth. In particular, there exists an optimal positive chirp which maximizes the spectral bandwidth, corresponding to the formation of single long-wavelength Raman soliton with almost all of the pump energy. These results provide a convenient means to significantly extend the wavelength range over which femtosecond pulses can be generated with a Ti:sapphire laser.

Numerical solutions to the one-dimensional nonlinear envelope equation including higher-order nonlinear effects were found using a standard split-step Fourier algorithm. For an input Gaussian pulse with an initial pulse chirp C_p of the amplitude $A(z=0,\tau) = A_0\exp(-(1+iC_p)\tau^2/2)$, the equation for the normalized amplitude $u(\xi,\tau) = A(\xi,\tau)/A_0$ can be expressed as[10]

$$\frac{\partial u(\xi,\tau)}{\partial \xi} = -\overbrace{\sum_{n\geq 2}\frac{i^{n-1}}{n!}\frac{L_{ds}}{L_{ds}^{(n)}}\frac{\partial^n u}{\partial \tau^n}}^{\text{Dispersion}}$$

$$+ i\frac{L_{ds}}{L_{nl}}\Big[(1-f_R)\Big(\overbrace{|u|^2 u}^{\text{SPM}} + \overbrace{\frac{i}{\omega_0\tau_p}\frac{\partial}{\partial\tau}(|u|^2 u)}^{\text{Self-Steepening}}\Big)$$

* Supported by the Hundred-Talent Project and the Knowledge Innovation Foundation of Chinese Academy of Sciences of China.

** Email: ccfu@mail.siom.ac.cn

©2004 Chinese Physical Society and IOP Publishing Ltd

$$+ \overbrace{f_R\Big(1+\frac{i}{\omega_0\tau_p}\frac{\partial}{\partial\tau}\Big)\Big(u\int_0^\infty h_R(\tau')|u(\xi,\tau-\tau')|^2d\tau'\Big)}^{\text{SRS}}\Big], \quad (1)$$

where the last two terms are of nonlinearity, $L_{ds}^{(n)} = \tau_p^n/\beta_n$ is the nth-order dispersion length, τ_p is the half-width (at $1/e$ intensity point) of a pulse that is related to the full width at half maximum (FWHM) $T_{\rm FWHM}$ by $\tau_p = T_{\rm FWHM}/1.665$ for a Gaussian pulse, $\beta_n (n \geq 2)$ is the nth-order dispersion constant, $L_{ds} = |L_{ds}^{(2)}|$ is the dispersion length, and $\xi = z/L_{ds}$ is the normalized distance. The normalized retarded time is $\tau = (t - z/v_g)/\tau_p$ for the pulse travelling at a group velocity v_g, $L_{nl} = 1/\gamma P_0$ is the nonlinear length, P_0 is the input pulse peak power, $\gamma = n_2\omega_0/cA_{\rm eff}$ is the nonlinearity coefficient, n_2 is the nonlinear refractive-index coefficient of the fused-silica glass, $A_{\rm eff}$ is the effective core area; $f_R = 0.18$ is the relative strength of the Raman contribution[10] and $u(\varsigma, \tau)$ is the normalized amplitude. The nonlinear susceptibility has two dominant time scales: a fast component that contributes to self-phase modulation (SPM) and four-wave mixing (FWM), and a slow component that is the origin of stimulated Raman scattering (SRS). Since the initial pulse duration in the simulations is 200 fs, the fast component of the response is treated as instantaneous while the non-instantaneous portion of the response is written in terms of the SRS temporal response $h_R(t)$, which is approximated by[10]

$$h_R(t) = \frac{\tau_1^2+\tau_2^2}{\tau_1\tau_2^2}\exp(-t/\tau_2)\sin(t/\tau_1), \quad (2)$$

with τ_1 and τ_2 taken to be 12.2 fs and 32 fs, respectively.[10] Thus Eq. (1) includes the effects of dispersion, self-phase modulation, self-steeping (SST), and intrapulse stimulated Raman scattering (ISRS).

In this Letter, we have simulated the nonlinear propagation and tunable femtosecond Raman soliton generation in the anomalous dispersion region of a PCF pumped by an initially 200-fs (FWHM) linearly polarized pulse. The PCF with a core diameter of 2 μm exhibits a significant waveguide contribution to the dispersion because of a large core-cladding index difference.[11,12] Only a single transverse mode can be excited in the fibre for wavelengths from 500 to 1600 nm. The zero-dispersion wavelength of the fibre is located at 767 nm. The specific values used are as follows: $n_2 = 3\times10^{-20}\,{\rm m^2/W}$, $A_{\rm eff} = 3.14\ (\mu{\rm m}^2)$, $\gamma = 0.075\,({\rm Wm})^{-1}$, $\omega_0\tau_p = 283.03$, $L_{ds} = 240.49\,{\rm cm}$, $L_{ds}/L_{ds}^{(3)} = 8.39\times10^{-2}$, $L_{ds}/L_{ds}^{(4)} = -3.89\times10^{-4}$, $L_{ds}/L_{ds}^{(5)} = 4.61\times10^{-6}$, $L_{ds}/L_{ds}^{(6)} = -2.64\times10^{-7}$. We have $L_{ds}/L_{nl} = 36.07$, 54.11, 72.15 for a peak power of 200 W, 300 W, 400 W, respectively. We retain terms up to the 6th order in the Taylor expansion of the propagation constant, which ensures the accuracy of the calculation and the fibre loss is neglected since only a short length of the fibre is considered in simulations.

The results for the pulse without an initial chirp are illustrated in the trace of spectral development with propagation distance (ξ) in Fig. 1(a). In the case of low power ($P_0 = 200\,{\rm W}$) and short propagation distance, the pulse exhibits asymmetric spectral broadening as a result of third-order dispersion, SPM, and SST. Subsequently, a peak appears in the spectrum at the blue side [see Fig. 1(a)]. A Raman soliton is formed after $\xi = 0.16$. The soliton is further red-shifted due to continuous intrapulse stimulated Raman scattering, which is related to the soliton self-frequency shift.[13] The corresponding time-domain behaviour is shown in Fig. 1(b), the pulse is initially compressed due to the combined effects of the nonlinearities and the anomalous dispersion before it breaks into multiple solitons. The time trace includes several delayed pulse components, corresponding to the red-shifted Raman solitons. The delays increase with the propagation distance and thus with the frequency shift. This is due to a decrease of the group velocity as the solitons shift towards the infrared. As is expected, the multiple solitons have different amplitudes with the soliton experiencing the largest delay exhibiting the largest amplitude. The pulses have a soliton-type profile, which indicates that the delayed pulses have a fundamental soliton nature. For a pulse of width $T_{\rm FWHM} = 200\,{\rm fs}$, the dispersion length of the fibre is equal to $L_D = \tau_p^2/\beta_2 = 240.49\,{\rm cm}$ at 800 nm, the nonlinear length $L_{nl} = 1/\gamma P_0 = 6.67\,{\rm cm}$ for the input peak power $P_0 = 200\,{\rm W}$. Consequently, the nonlinear length is shorter than L_D and the pulse launched into the fibre corresponds to an Nth-order bound-state soliton. Such a soliton is constituted of N fundamental solitons (N is the nearest integer for $\sqrt{L_D/L_{NL}} = \tau_p\sqrt{\gamma P_0/|\beta_2|}$), whose relative group velocities and amplitudes are given by the real and imaginary parts of the eigenvalues obtained by solving the simplified nonlinear Schrödinger equation using the inverse scattering method.[14] The amplitudes and widths of the individual constituents can be expressed as[14]

$$A_k = \frac{A_0(2A_0-2k+1)}{N}, \quad T_k = \frac{T_0}{2A_0-2k+1},$$

with $k \in [1, N]$ and A_0 being equal to $\sqrt{P_0}$. In the absence of perturbation, i.e. when the higher-order dispersion (HOD) and SRS terms are neglected, the real parts of the eigenvalues are degenerate and the Nth-order soliton is a bound-state that propagates with periodical changes in its spectrum. The HOD and SRS terms tend to break the degeneracy of the eigenvalues making the different constituents travel with different group velocities. Therefore, the bound-state of the Nth-order soliton is broken and the initial pulse decays into several sub-pulses which propagate independently as fundamental solitons. Even though HOD can lead to soliton decay by itself, we found that the threshold is lower for SRS than for HOD to induce the

decay in the case of femtosecond pulses and our used PCFs. In other words, the soliton decay is primarily due to stimulated Raman scattering.[15] The solitons all undergo soliton self-frequency shift. Therefore, they appear in the spectrum as distinct red-shifted components. The solitons are perturbed by HOD as they propagate along the PCF. As a consequence, they radiate energy in order to maintain their shape. This radiated energy appears in the spectrum as anti-Stokes peaks. They are generated with a much lower intensity than the Stokes lines that correspond to the Raman solitons[9] as shown in Fig. 2. The Stokes and anti-Stokes lines gradually shift further into the red and blue, respectively, as the input power increases. When the peak power increases up to 400 W, clean discrete self-frequency shifted solitons are formed and readily tuned over 210 nm. The corresponding time-domain behaviour becomes highly complex, with the initial pulse breaking up into numerous pulses, some of which are even compressed to sub-40-fs pulses as seen in Fig. 3, much shorter than those reported previously with similar pulse duration and pulse energy in conventional fibres.[7,8] We attribute this to the small mode size and the large anomalous dispersion and small cubic dispersion effect in the PCF. Those results are in good agreement between our simulation results and recent experimental observation.[6,13]

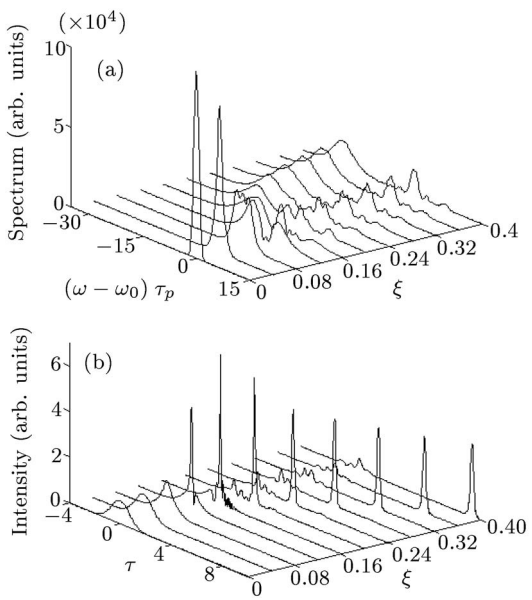


Fig. 1. Plots of (a) the spectra and (b) the temporal shape of a femtosecond pulse as a function of normalized distance along a photonic crystal fibre for the pump wavelength ($\lambda_p = 800$ nm) located in the anomalous dispersion region and the input peak power $P_0 = 200$ W.

The effect of the initial pulse chirp on the spectral bandwidth is shown in Fig. 4 for five typical chirps of $C_p = -5$, 0, 5, 10, and 20 (indicated as A, B, C, D and E, respectively) for the constant peak power of 400 W with fibre length of only 57.5 cm. From Figs. 4(a) and 4(b), we can see clearly how the temporal and spectrum intensity change due to different chirps. Spectral bandwidth increases with the chirp parameter C_p in an essentially monotonic fashion until the optimal chirp. The reason that spectral bandwidths increases with the chirp parameter C_p can be explained as follows. A positive initial chirp adds to the chirp created by SPM near the pulse centre, thus enhances the initial pulse compression and obtains higher peak power, enhancing the continuum generation and creating a

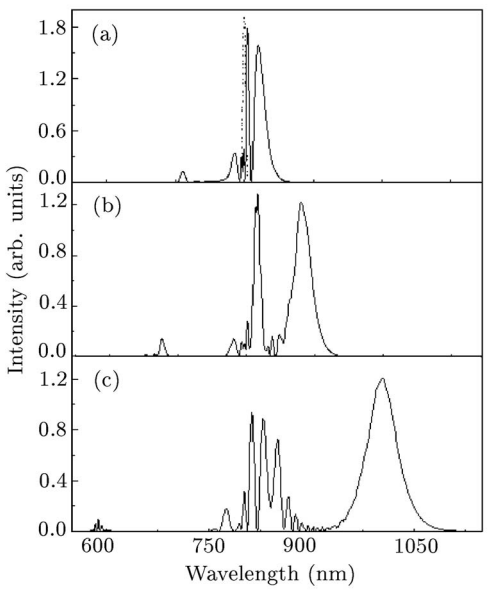


Fig. 2. A set of output spectra and input spectra (dashed curve) obtained with 200-fs 800 nm pulses for increasing input peak powers P_0: (a) $P_0 = 200$ W, (b) $P_0 = 300$ W, (c) $P_0 = 400$ W at a constant propagating distance $\xi = 0.16$.

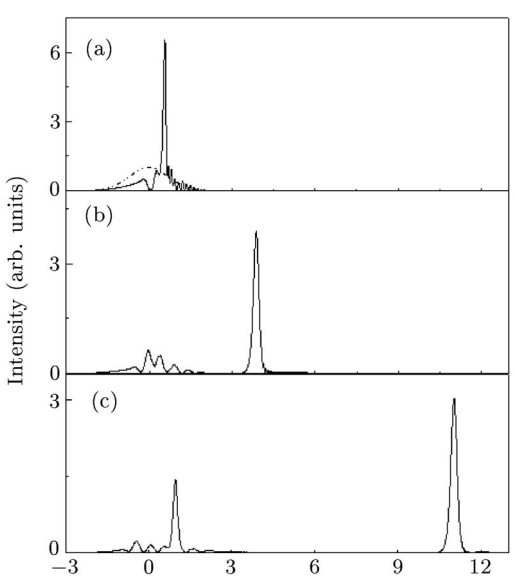


Fig. 3. A set of output temporal shape and input temporal shape (dashed curve) obtained with 200-fs 800 nm pulses for increasing input peak powers P_0: (a) $P_0 = 200$ W, (b) $P_0 = 300$ W, (c) $P_0 = 400$ W at a constant propagating distance $\xi = 0.16$.

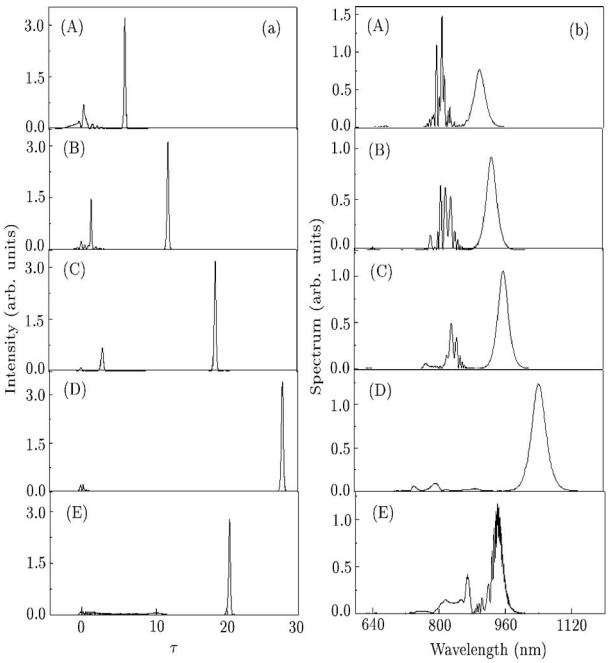


Fig. 4. Effect of the initial pulse chirp on the spectral bandwidths: (a) temporal shape, (b) spectrum for varying initial pulse chirp $C_p = -5$, 0, 5, 10, 20 labelled respectively as A, B, C, D and E. The fibre length $L = 57.5$ cm, the input peak power $P_0 = 400$ W.

broader spectrum. In contrast, a negative initial chirp reduces the effect of SPM by cancelling the frequency chirps near the pulse centre, diminishing the pulse compression and thus creating a narrower spectrum. The most interesting effect of the chirp is that there exists an optimal positive chirp that maximizes the spectral bandwidth. From Figs. 4(a) and 4(b), we can compare the different characteristics of spectrum obtained with pulses of different chirps near the optimal value. With the optimal chirp of $C_p = 10$, the spectrum reaches the maximum bandwidth. Here we obtained a sub-40-fs width, tunable over 244 nm Raman soliton with almost all of pumping energy. In contrast, when the chirp deviates from the optimal value, the spectra bandwidth decreases. The reason that there exists an optimal positive chirp can be explained as follows. For pulse widths ~ 200 fs, the spectral width of the pulse is large enough so that the Raman gain can amplify the low frequency (red) spectral components of the pulse with the high-frequency (blue) components of the same pulse acting as a pump. With a large initial pulse chirp, the bandwidth of the input pulse is broad enough to have more spectral components within the Raman amplification bandwidth. Therefore, SRS plays an increasingly important role as the initial pulse chirp increases. That is to say, the initial pulse chirp can enhance the energy transfer and thus almost all of the pumping energy is transferred to the Raman soliton at the optimal chirp as shown in Fig. 4b(D). Since the Raman soliton obtains the almost all of pumping energy and thus enhances the nonlinear effects in a PCF, which causes the Raman soliton to reach the maximal frequency shift. On the other hand, the increasing power of Raman soliton causes the effects of HOD to start to play a larger role in suppressing the Raman gain. Therefore, when the initial pulse chirp further increases, the Raman soliton radiates energy due to the effects of HOD in order to maintain its shape. This radiated energy appears in the spectrum as a dispersive wave as shown in Fig. 4b(E).[16] This emission will reduce the energy of the Raman soliton and thus cause the frequency shift to increase no more.

In conclusion, we have theoretically demonstrated a widely tunable soliton source in a PCF pumped by 200-fs pulse. It is found that the output wavelength can be widely tuned by varying the input peak power or the initial pulse chirp parameter C_p. We obtained solitons with a sub-40-fs width, tunable over a range from 800 to 1044 nm with a photonic crystal fibre only 57.5 cm long but highly nonlinear. In particular, the simulations show that there exists an optimal chirp value that maximizes the spectral bandwidth, corresponding to the formation of single long-wavelength fundamental soliton. This formation of single long-wavelength Raman soliton with almost all of pumping energy is somewhat more desirable than multiple solitons. As an important parameter, the initial pulse chirp could be used together with other parameters to obtain a desirable widely tunable spectrum. These results provide a convenient means to significantly extend the wavelength range over which femtosecond pulses can be generated with Ti:sapphire laser. We anticipate that PCFs will find similar applications with other near-infrared femtosecond pulse sources.

References

[1] Ranka J K et al 2000 *Opt. Lett.* **25** 25
[2] Birks T A et al 1997 *Opt. Lett.* **22** 961
[3] Broeng J et al 1999 *Opt. Fibre Technol.* **5** 305
[4] Jones D J et al 20000 *Science* **288** 635
[5] Hartl I et al 2001 *Opt. Lett.* **26** 608
[6] Liu X, Xu C and Knox W H 2001 *Opt. Lett.* **26** 358
[7] Nishizawa N and Goto T 1999 *IEEE Photon. Technol. Lett.* **11** 325
[8] Fermann M E et al 1999 *Opt. Lett.* **24** 1428
[9] Beaud P et al 1987 *IEEE J. Quantum Electron.* **23** 1938
[10] Agrawall G P 2001 *Nonlinear Fibre Optics* (New York: Academic)
[11] Knight J C, Birks T A and Russell St J 1998 *J. Opt. Soc. Am.* A **15** 748
[12] Li S G, Hou L T and Fan D Y 2003 *Chin. Phys. Lett.* **20** 1300
[13] Washburn B R, Ralph S E and Dudley J M 2002 *Electron. Lett.* **37** 1510
[14] Kodama Y and Hasegawa A 1987 *IEEE J. Quantum Electron.* **23** 510
[15] Wen S C, Su W H and Fan D Y 2003 *Chin. Phys. Lett.* **20** 852
[16] Herrmann J, Griebner U and Korn J 2002 *Phys. Rev. Lett.* **88** 173901